ENCLOSURE 1

ADDITIONAL INFORMATION ON RACK-TO-RACK INTERACTIONS

(Nonproprietary Version)

DIABLO CANYON POWER PLANT

UNITS 1 AND 2

ADDITIONAL INFORMATION ON RACK-TO-RACK INTERACTIONS

(Nonproprietary Version)

Pacific Gas and Electric Company

April 7, 1987

1374S/0049K

TABLE OF CONTENTS

[illegible]

1. INTRODUCTION

In response to NRC Staff requests, PGandE submitted additional information on spent fuel rack interaction parametric studies on February 6, 1987 (PGandE Letter No. DCL-87-022). On February 18, 1987, the Staff and PGandE met to discuss the parametric studies. Following the meeting, the Staff requested additional information, which necessitated further investigations (NRC Letter dated February 26, 1987). These further parametric studies and their results were reviewed by the Staff on March 26, 1987. This report documents the description and results of the additional parametric studies that were presented to the Staff at the March 26 technical review meeting and also responds to the Staff's information requests dated February 11 and 26, 1987.

In response to these Staff requests, rocking, a lower coefficient of friction, fluid coupling effects, and variations in fabrication and installation tolerances were incorporated in the parametric studies. As specified by the Staff, resultant fuel-to-rack, rack-to-rack, and rack-to-wall forces were compared for the single-rack and multi-rack models. Time-history data have been provided in this report.

2. BACKGROUND OF DESIGN BASIS ANALYSIS

The analytical methodology used for obtaining rack interaction impact loads is described in the Reracking Report submitted by PGandE on September 19, 1985 (Reference 1). In general, the methodology includes several conservative assumptions applied to a single rack model to obtain conservative impact loads which were used as the basis for rack qualification. Some of these conservative assumptions are listed below:

- Each adjacent rack module was assumed to move in a manner equal and opposite (out of phase) to the rack module being analyzed. This assumption was incorporated in the model by utilizing a reference impact plane midway between adjacent racks.

- The fluid coupling coefficients were based on the conservative assumption that adjacent rows of racks are an infinite distance away (the distance is measured perpendicular to the horizontal ground motion). This neglects the cross-coupling effect of the adjacent rows of racks and results in higher displacements and impact forces.

- The impact spring coefficients were set at a value significantly higher (over 10 times) than the calculated values to produce conservative impact forces.

- All hydrodynamic coupling calculations were conservatively based on the initial gap. Parametric studies showed that progressive time-dependent variation of gaps (nonlinear coupling), if considered, would further reduce rack responses.

- The friction coefficients used were 0.2 and 0.8.

The racks and fuel were analyzed using an eight degree-of-freedom system to model their three-dimensional behavior during an earthquake.

It was PGandE's judgment that the above conservatisms, when used in a single-rack analysis, provide an adequate design basis to accommodate multi-rack impact effects.

The results of PGandE's design basis analysis, as reported in the Reracking Report, demonstrate conservative design margins between predicted and allowable loads. Tables 2-1 and 2-2 summarize the maximum impact loads and the qualification basis of the racks, as reported in the Reracking Report, the Seismic Analysis Report (Reference 2), and other supporting documentation.

3. DESCRIPTION OF TWO-DIMENSIONAL PARAMETRIC STUDIES

The objective of the parametric studies reported herein is to show quantitatively that PGandE's methodology for obtaining the design basis impact loads, reported in the Reracking Report, is conservative. These studies were performed by the same group of individuals who performed the original analysis. Additionally, all work was reviewed and accepted by PGandE to assure the accuracy and completeness of the evaluations.

3.1 SINGLE-RACK MODEL

The single-rack model (Figure 3-1) was developed for a 10 x 10 rack module fully loaded with fuel. Consistent with the design basis model, 40 percent of the fuel mass was modeled as one lumped mass (Mass A) located near the top of the rack to simulate the rattling effect of the fuel assemblies. The balance of the fuel mass was located at the base of the rack. The mass of the rack was lumped at the centroid of the rack. The rattling mass was assigned a translational degree-of-freedom; the rack centroid was represented by three degrees-of-freedom (translational, vertical, and rocking).

Two cases were studied using the single rack-model. In the first case, all model parameters were set at the same conservative values as those reported in the Reracking Report. This case was used to develop benchmark loads for comparison with other cases, since it represented PGandE's conservative analysis input for a two-dimensional model.

In the second case the model parameters were revised to represent realistic input values as follows:

- In calculating the fluid coupling coefficient, the presence of adjacent rows of racks was accounted for by considering them as vertical planes located at a lateral distance 7.5 inches on either side of the rack (versus the nominal 2.25-inch gap between two adjacent arrays). Analytical studies have shown that use of a 7.5-inch gap is conservative (see Section 5 of this report).

- Both the rattling springs and the exterior impact springs were represented by their calculated values scaled up (approximately 1-1/2 times) to account for strain rate and material variability.

3.2 MULTI-RACK MODEL

Two rack arrays were studied. These arrays are identified as Sections AA and BB in Figure 3-2. The array identified by Section AA was selected to study the behavior of a typical interior row, whereas the second array (Section BB) was selected to study the behavior of a row of racks with a gap larger than 7.5 inches, which occurs along the periphery of the spent fuel pool.

Figure 3-3 shows the two-dimensional dynamic model used in the analysis of the racks in Section AA. A similar model was developed for Section BB. [

] The parameters for the model were developed in a manner similar to that used for the single-rack model, except that more realistic assumptions were made to compute the fluid coupling coefficients and spring constants, as follows:

- In calculating the fluid coupling coefficients for Section AA, the presence of adjacent rows of racks was accounted for by considering them as vertical planes located at a lateral distance of 7.5 inches on either side of the rack array (versus the nominal 2.25-inch gap between adjacent rack module walls). Analytical studies showed that the 7.5-inch gap (h_0) conservatively estimates the coupling effects of adjacent rack arrays (see Section 5 of this report).

  For Section BB, fluid coupling coefficients were developed by conservatively assuming that the adjacent wall is approximately 37 inches away from all racks in the array. This assumption of uniform channel width was made to simplify the analysis, and it is conservative, as only one out of four racks is approximately 37 inches away from the wall and the other three are much closer to the wall.

- Both the rattling springs and the exterior impact springs were represented by their calculated values scaled up (approximately 1-1/2 times) to account for strain rate and material variability.

The Hosgri east-west and vertical ground motions were applied simultaneously to the model. The east-west horizontal time-histories were applied since they represent the most conservative horizontal seismic input.

The key model parameters are summarized in Tables 3-1 and 3-2.

3.3 CASES STUDIED

Table 3-3 summarizes the description and objective of each case studied. In general, these cases were selected to study the following:

- Conservatism in PGandE's design basis methodology using a two-dimensional, single-rack model

- Comparison of multi-rack response with the single-rack response determined using PGandE's design basis methodology

- Effects of full and empty racks (11 assemblies)

- Effects of larger lateral gaps [ ] on rack response

- Effects of manufacturing tolerances on rack response

4. ANALYTICAL METHODOLOGY

The analytical methodology is similar to the one described by Levy and Wilkinson, (Reference 3). In general, the analysis includes the following steps:

<u>Step 1</u>: The system kinetic energy was calculated considering the combined effects of the following:

[

•

•

•

•

•

]

<u>Step 2</u>: After the system kinetic energy was developed, [ ] equation of motion was used to solve for the fluid reaction force:

[ ]

Step 3: The equations of motion developed in Step 2 were solved using the computer code DYNAHIS, which employs a nonlinear, time-history analysis using a central difference integration technique. Additional discussions of DYNAHIS were provided to the NRC during the review of the Reracking Report.

5. HYDRODYNAMIC COUPLING

5.1 DEVELOPMENT OF EXTERNAL COUPLING TERMS

5.2 PARAMETRIC STUDIES FOR EQUIVALENT LATERAL GAP (h_0)

5.3 EFFECTS OF VERTICAL FLOW

5.4 MODELING OF FUEL ASSEMBLIES

The PWR fuel assemblies used in the Diablo Canyon Unit 1 and 2 reactors contain 264 fuel rods in a 17 x 17 array. The fuel rods are 0.374 inches in diameter arranged in a square lattice with a pitch of 0.496 inches. Therefore, the gap between the adjacent fuel rods is less than 1/8 inch (0.122 inches nominal). The cross-sectional dimension of the rod array is 8.404 inches square. Since the storage cell opening cross-sectional dimension is 8.85 inches, the net lateral spacing between the fuel assembly and the storage cell is 0.446 inches. The lateral movement of the fuel assembly in the storage cell causes the water to flow past the assembly. Since the flow between these narrow channels formed by the array of rods involves repeated changes in the flow cross-section of width from 0.122 inches to 0.496 inches - a fourfold change in transverse flow area - the hydraulic pressure losses through these channels are an order of magnitude greater than what the fluid encounters flowing through the assembly/cell wall gap. The hydraulic pressure loss due to flow through these narrow convergent/divergent channels is an important mechanism for energy loss from the vibrating rack system. However, in the conservative approach used to model fluid coupling, no such flow, and therefore, no such loss occurs; all the fluid is assumed to flow in the assembly/cell wall space.

6. RESULTS OF ANALYSES

6.1 SINGLE RACK

Table 6-1 summarizes the maximum impact loads for parametric Cases 1 and 2.

Therefore, the results of Case 1 show that PGandE's design basis methodology is conservative.

Figures 6-1 through 6-4 provide time-history plots of the rack translation and wall impact forces as obtained from Case 1.

[illegible]

[illegible]

[illegible]

[illegible]

[illegible]

[illegible] [illegible]

[illegible]

[illegible]

[illegible]

[illegible]

[illegible]

[illegible]

[illegible]

[illegible]

6.2 MULTI-RACK INTERACTIONS

6.2.1 Interior Rack Array

Table 6-2 shows the results of the multi-rack analyses. Cases 3 and 4 represent analyses of the interior array identified by Section AA. These cases were chosen to predict rack behavior under different loading configurations. Case 3 represents an array of four fully loaded racks, and Case 4 represents three loaded racks and one empty rack (11 fuel assemblies). The results show that for both cases the fuel-to-rack and rack-to-rack impact loads are enveloped by Case 1, which reflects the results based on the conservative design methodology employed by PGandE. Although rack-to-wall loads based on Cases 3 and 4 are greater than the corresponding loads obtained from Case 1, their magnitude is enveloped by the rack-to-rack load resulting from Case 1.

Figures 6-5 through 6-17 show typical time-history plots of rack translation and wall impact forces for Case 3.

6.2.2 Exterior Rack Array

Section BB was chosen for analysis to quantify the effects on rack behavior in the few cases where spacing between the rack and the wall exceeds 7.5 inches.

The results of the analysis (Table 6-2) show that the fuel-to-rack and rack-to-rack impact forces are enveloped by Case 1.

6.2.3 Fabrication and Installation Tolerances

Table 6-3 provides results of the multi-rack analyses which postulated variable gaps resulting from fabrication and installation tolerances. The results show that the fuel-to-rack and rack-to-rack impact forces are enveloped by the corresponding loads obtained from Case 1, and that rack behavior is not sensitive to typical fabrication tolerances.

7. CONCLUSIONS

In conclusion, the two-dimensional parametric studies demonstrate that the use of conservative springs and fluid coupling inputs in the Reracking Report yield conservative rack and fuel assembly impact loads. These studies provide a high level of confidence that the design basis model has predicted conservative rack qualification loads, which ensures compliance with all design criteria. Table 7-1 summarizes these loads.

8. REFERENCES

1. Reracking of Spent Fuel Pools, Diablo Canyon Units 1 and 2, Enclosure to PGandE Letter No. DCL-85-306, dated September 19, 1985.

2. Seismic Analysis Report, "Seismic Analysis of High Density Fuel Racks for Pacific Gas and Electric for Diablo Canyon Nuclear Power Station," Rev. 3, September 3, 1986, A. Soler, TM #779.

3. Levy, S., and Wilkinson, J.P.D., The Component Element Method in Dynamics with Applications to Earthquake and Vehicle Engineering, McGraw-Hill, New York, 1976.

4. Lamb, H., Hydrodynamics, Dover Publications, New York, 1945.

5. Fritz, R. J., "The Effects of Liquids on the Dynamic Motions of Immersed Solids," Journal of Engineering for Industry, Trans. of the ASME, February 1972, pp. 167-172.

TABLE 2-1

Results of Design Basis Analysis
(Single Rack, 8 Degrees-of-Freedom)

Friction Coefficient	Impact Loads (Kips)[a]		
	F_{rf}	F_{rr}	F_{rw}
$\mu = 0.8$	249	88	39[b]
$\mu = 0.2$	242	105[b]	63[c]

a. F_{rf} is the rack-to-fuel impact load; F_{rr} is the rack-to-rack impact load; F_{rw} is the rack-to-wall impact load.

b. The maximum load resulted from an empty rack (11 fuel assemblies).

c. The value applies to rack "H" only.

TABLE 2-2

Qualification Basis for Racks
(Reracking Report)

Impact Location	Allowable Load (Kips)[a]
Fuel-to-rack	883
Rack-to-rack	175[b]
Rack-to-wall	175 for rack[b] 80 for wall[c]

---

a. The allowable loads refer to a 10 x 11 rack.

b. The loads correspond to the allowables per spring. Both the girdle bars and baseplate are represented by two springs each.

c. The walls have been shown to be qualified for substantially larger (≈200 kips) loads.

TABLE 3-1

Key Model Parameters
(Single-rack Model)

A. SPRING CONSTANTS

1. Fuel-to-Rack

   a. Springs 3, 4

2. Rack-to-Rack/Rack-to-Wall

   a. Girdle bars:

      Springs 1 and 2

   b. Baseplate:

      Springs 5 and 6

B. GAPS

1. Rack-to-Rack

2. Rack-to-Wall

3. Fuel Assemblies to Cells

TABLE 3-2

Key Model Parameters
(Multi-rack Model)

A. SPRING CONSTANTS

1. Fuel-to-Rack

2. Rack-to-Rack

   Girdle bars
   Baseplate

3. Rack-to-Wall

   Girdle bars
   Baseplate

B. GAPS

1. Rack-to-Rack

2. Rack-to-Wall

3. Fuel Assemblies to Cells

TABLE 3-3

Description of Cases Studied

Case No.	Model	Degrees-of-Freedom	Description	Objective
1				
2				
3				
4				
5				
6				
7				

TABLE 5-1 SUMMARY OF PARAMETRIC STUDIES FOR EQUIVALENT LATERAL GAP

[illegible]ES	DESCRIPTION	LATERAL GAP

TABLE 6-1

Summary of Single Rack Results

Case	Description	Impact Loads (Kips)[a] F_{rf}	F_{rr}	F_{rw}
1				
2				

a. F_{rf} is the maximum rack-to-fuel impact load as represented by springs 3 and 4 (Figure 3-1); F_{rr} is the maximum rack-to-rack impact load as represented by springs 2 and 6; F_{rw} is the maximum rack-to-wall impact load as represented by springs 1 and 5.

TABLE 6-2

Summary of Multi-rack Results Analysis

Case	Description	Impact Loads (Kips)[a] F_{rf}	F_{rr}	F_{rw}
3				
4				
5				

a. F_{rf} is the maximum rack-to-fuel impact load as represented by springs 3 and 4 (Figure 3-2); F_{rr} is the maximum rack-to-rack impact load as represented by springs 2 and 6; F_{rw} is the maximum rack-to-wall impact load as represented by springs 1 and 5.

TABLE 6-3

Summary of Multirack Results
(Effect of Tolerances)

Cases	Description	Impact Loads (Kips)(a) F_{rf}	F_{rr}	F_{rw}
6				
7				

---

a. F_{rf} is the maximum rack-to-fuel impact load as represented by springs 3 and 4 (Figure 3-2); F_{rr} is the maximum rack-to-rack impact load as represented by springs 2 and 6; F_{rw} is the maximum rack-to-wall impact load as represented by springs 1 and 5.

b.

c.

TABLE 7-1

MAXIMUM LOADS

Case	Rack Model[a]	Assumption[b]	Rack Impact Loads Fuel[c]	Rack Impact Loads Rack[d]
Licensing Basis	SR	C	249	105
1	SR	C		
2	SR	R		
3	MR	R		
4	MR	R		
5	MR	R		
6	MR	R		
7	MR	R		
Allowables			883[e]	175(r) 200(w)

(a) SR = Single Rack Analysis, MR = Multiple Rack Analysis

(b) C = Conservative Assumptions Used in Analysis (high spring constants and large hydrodynamic gaps)
R = Realistic Assumptions Used in Analysis

(c) Maximum fuel impact load (rack-to-fuel), all loads in kips

(d) Maximum of rack-to-rack or rack-to-wall loads, all loads in kips

(e) Allowable for 10 X 11 rack; Allowable for 10 X 10 rack is 803; (r) = rack and (w) = wall

Fig. 3-1 FOUR DEGREE-OF-FREEDOM SINGLE RACK/FUEL ASSEMBLY MODEL

[illegible]

[illegible]

[illegible]

[illegible]

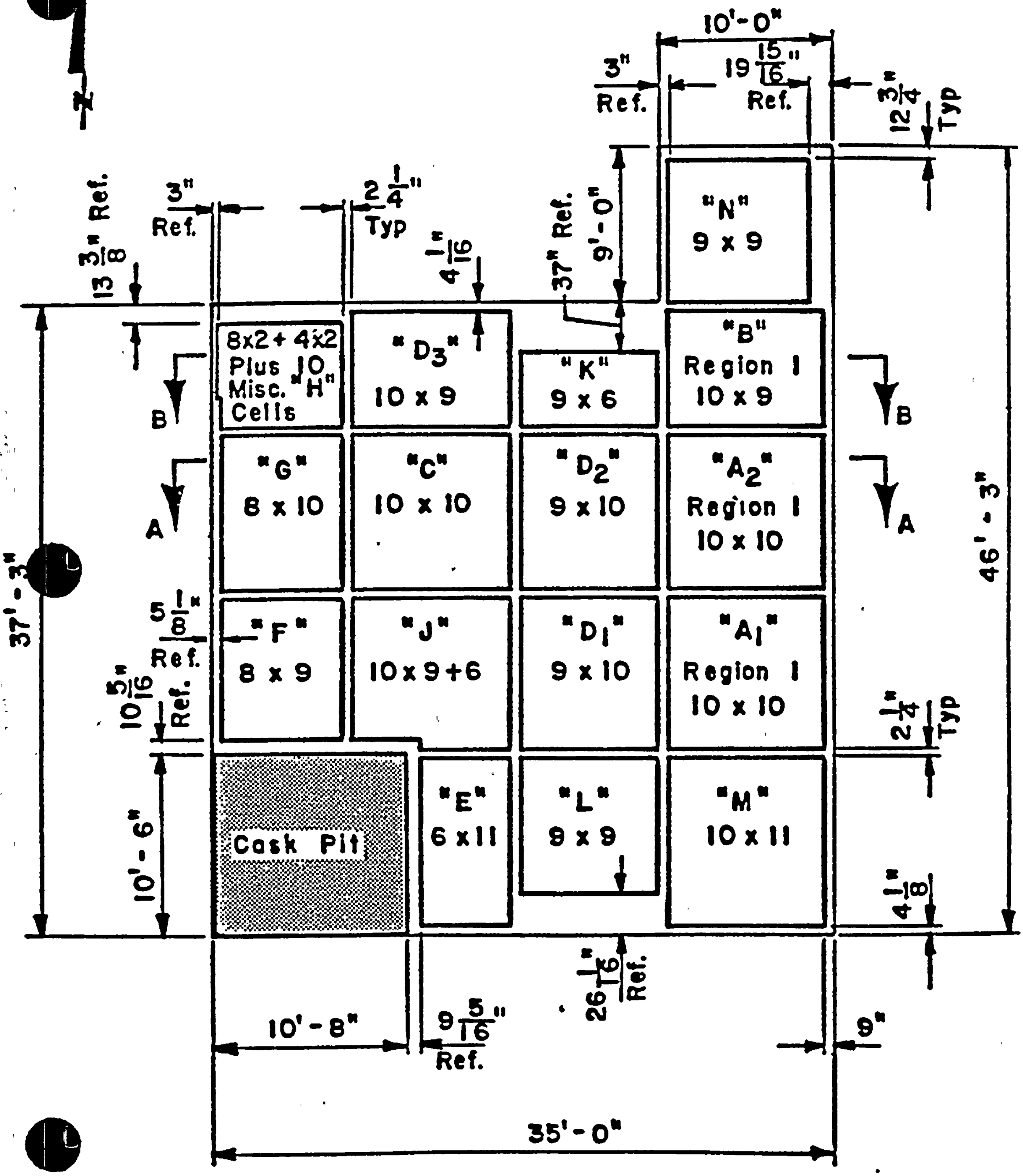

Fig. 3-2 Typical Layout of Unit 1 Spent Fuel Pool

Fig. 3-3 MULTI-RACK MODEL, EAST-WEST ARRAY, HOSGRI EARTHQUAKE

Fig. 5-1 Typical Four Rack Array
Used for Hydrodynamic Coupling

FIG. 5-2 DISTRIBUTION OF FLOW BETWEEN RACKS

Fig. 5-3 Distribution of Flow Between Fuel Assemblies and Cells

(See Fig 5-2 for Notes)

Figure 6-1 Rack Translation for Case 1 [ ] [ ]

Figure 6-2 Rack Translation for Case 1[ ]

[ ]

Figure 6-3   Rack to Rack Impact Force Case 1 [ ]
[ ]

Figure 6-4   Rack to Rack Impact Force for Case 1 [ ]
[ ]

1365S/0049K

Figure 6-5 Rack Translation for Case 3 [ ]
[ ]

Figure 6-6 Rack Translation for Case 3 [ ]
[ ]

Figure 6-7 Rack Translation for Case 3 [ ]
[ ]

Figure 6-8 Rack Translation for Case 3 [ ]
[ ]

Figure 6-9 Rack to Wall Impact Force for Case 3 [ ]
[ ]

[illegible]

[illegible]

Figure 6-10 Rack to Wall Impact Force for Case 3 [ ]
[ ]

Figure 6-11 Rack to Wall Impact Force for Case 3 [ ]
[ ]

Figure 6-12 Rack Translation for Case 3 [ ]

[ ]

Figure 6-13 Rack Translation for Case 3 [ ]
[ ]

Figure 6-14 Rack Translation for Case 3 [ ]

[ ]

1365S/0049K

Figure 6-15 Rack Translation for Case 3 [ ]

[ ]

[ ]

Figure 6-16 Rack to Wall Impact Force for Case 3 [ ]

[ ]

Figure 6-17 Rack to Wall Impact Force for Case 3 [ ]

[ ]